New CMB spectral distortion constraints on decaying dark matter with full evolution of electromagnetic cascades before recombination

Sandeep Kumar Acharya* and Rishi Khatri†

Department of Theoretical Physics, Tata Institute of Fundamental Research, Mumbai 400005, India

(Received 12 March 2019; published 12 June 2019)

Current constraints on energy injection in the form of energetic particles before the epoch of recombination using CMB spectral distortions assume that all energy goes into y and μ-type distortions. We revisit these constraints with exact calculations of the spectral distortions by evolving the electromagnetic cascades. The actual spectral distortion differs in shape and amplitude from the y-type distortion and depends on the energy and nature of injected particles. The constraints on the energy injection processes such as dark matter decay can be relaxed by as much as a factor of 5.

DOI: 10.1103/PhysRevD.99.123510

I. INTRODUCTION

In the standard ΛCDM cosmology, the cosmic microwave background (CMB) has an almost perfect blackbody spectrum, a consequence of almost complete thermal equilibrium in the early Universe. Any deviation from equilibrium in the CMB spectrum is exponentially suppressed at redshifts $z \gtrsim 2 \times 10^6$ [1–4]. The Planck spectrum once created is preserved by the expansion of the Universe. At redshifts $z \lesssim 2 \times 10^6$, it is no longer possible to restore the equilibrium disturbed by, for example, injection of energetic standard model particles such as photons, electrons, and positrons. It therefore becomes possible to create deviations in the CMB from a Planck spectrum. By observing these spectral distortions of the CMB, we can learn about the physical processes which injected energy into the CMB at $z \lesssim 2 \times 10^6$. The high entropy per baryon in our Universe, quantified by the photon-to-baryon number density ratio ($\sim 10^9$), means that the recombination dynamics is controlled by the energetic photons in the Wien tail of the Planck spectrum with the recombination starting only when the temperature of the CMB is more than a factor of 30 smaller than the Lyman-α energy [5,6]. As a result, the recombining and subsequent Universe, with most neutral atoms in the ground state, is optically thin to the bulk of the photons in the CMB since they are at energies much smaller compared to the energy of the first excited state of neutral atoms. The CMB spectral distortions, and the information about the energy injection processes in the early Universe, are therefore preserved through recombination and are observable today.

The measurement of the CMB monopole spectrum in the 1990s by the Far Infrared Absolute Spectrometer (FIRAS) onboard the Cosmic Background Explorer (COBE) satellite [7,8] remains the best constraint on the deviation of the CMB monopole spectrum from a blackbody until today. The COBE-FIRAS data has been used by numerous authors to constrain many exotic as well as standard model energy injection processes in the early Universe (e.g., [9–11], see [12] for a review). Almost all calculations until now have assumed that the injected energy ends up heating the electrons [1,3,13–17] irrespective of the initial energy or nature of the injected particles. The Compton scattering of CMB photons on heated electrons produces y-type distortions which then thermalize to i-type and μ-type (Bose-Einstein spectrum) distortions [16]. We will call y, i, and μ-type distortions collectively as yim-distortions and the assumption that all energy goes into heat or yim-distortions as the yim-approximation. The amplitude of the yim-distortions depends on the amount of energy injected while the shape depends on the redshift of energy injection, with departure from the y-type distortion becoming important at $z \gtrsim 10^4$. The information hidden beyond y and μ-type distortions, in the i-type distortions, has been explored previously by [16–19].

We have recently shown that this simple picture of yim-distortions is incomplete [20]. In particular, when the energy is injected in the form of standard model particles, with energy much greater than the average energy of the CMB photons, not all of the energy goes into the yim-distortions as is usually assumed. A significant fraction of energy is lost by the particles as they collide with the background electrons, ions, and photons and make their way down in energy toward thermalization with the background. The Compton scattering of relativistic electrons, produced in the cascade, with the CMB results in spectral distortions with distinctly different shape and amplitude compared to the yim-distortions. We call these distortions nonthermal relativistic or ntr-type spectral distortions.

*sandeepkumar@theory.tifr.res.in
†khatri@theory.tifr.res.in

The shape and amplitude of the *ntr*-type spectral distortions depend on the energy, type, and redshift of injected particles [20]. In particular, a fraction of the energy goes into the high frequency Wien tail of the spectral distortions resulting in decrease in the amplitude of the distortions in the main observable CMB frequency range compared to the *yim*-approximation. We therefore expect significant corrections to the existing constraints on energy injection scenarios in the early Universe.

A particularly interesting scenario which injects energetic particles is decay of unstable dark matter particles. The dark matter direct detection experiments, looking for weakly interacting massive particles (WIMPs) have so far not yielded any detection and the allowed parameter space for WIMPs is gradually being ruled out. This has motivated physicists to look beyond the simplest thermal WIMP models. One way around the direct detection constraints is super-WIMPs (SWIMP), where instead of producing the usual lightest stable particle in the theory in a beyond standard model theory like supersymmetry or Kaluza-Klein models, the thermally produced WIMP is the next-to-lightest particle which then decays to the lightest stable particle of the theory with the right abundance needed for dark matter [10,21]. For a review of dark matter models, see [22]. We can escape the direct detection constraints if the lightest particle, which would be the dark matter today, has much weaker interactions with the standard model particles, i.e., is a SWIMP. We could in general have additional unstable particles which were produced in the early Universe, with lifetime of a few years to hundreds of thousands of years, which would decay not into SWIMPs + standard model particles but completely into standard model particles. More generally, we would like to constrain the energy injection in the form of different standard model particles over the entire history of the Universe and look for deviations from standard cosmology as a probe of beyond standard model physics. Another interesting example of energy injection in the form of energetic photons and other particles is from evaporating primordial black holes [23] or from accreting primordial black holes [24–26]. We note that there are examples of long lived composite particles in the standard cosmology. During the big bang nucleosynthesis, tritium (^{3}H) and beryllium (^{7}Be) are produced which decay to stable isotopes of helium (^{3}He) and lithium (^{7}Li) at redshifts of $z_{^7\mathrm{Be}} = 3 \times 10^4$ and $z_{^3\mathrm{H}} = 2.5 \times 10^5$ respectively injecting energy into the CMB [27]. Unfortunately the abundance of these elements in our Universe is too low for the resulting spectral distortions to be observable.

We use Planck [28] ΛCDM cosmological parameters for all calculations and parameterize the injected energy, ρ_{X}, as a fraction of CDM dark matter density, $f_{\mathrm{X}} = \rho_{\mathrm{X}}/\rho_{\mathrm{CDM}}$, where ρ_{CDM} is the ΛCDM (nondecaying) dark matter density. When we consider only *yim*-distortions, f_{X} and lifetime τ_X or the corresponding redshift z_X are the only parameters that need to be considered. With the explicit evolution of electromagnetic cascades, the spectral distortions and constraints in addition become sensitive to the dark matter mass, m_X, as well as the decay channel or the initial spectrum of photons, electrons and positrons injected in the decay.

II. ELECTROMAGNETIC CASCADES IN THE EXPANDING UNIVERSE

In this work, we explicitly follow the electromagnetic cascade to calculate the *ntr* part of the distortion while keeping track of energy that is lost to heat to calculate the *yim*-type contribution to the total CMB spectral distortion resulting from the injection of energetic particles. When using COBE-FIRAS data, previous authors have approximated the full distortion with a y-type or μ-type distortion [9–11]. We note that even in the *all energy going to heat approximation* there is a small difference between the y- and μ-distortion from the actual *yim*-distortion for $10^4 \lesssim z \lesssim 2 \times 10^5$ [16]. We evolve even the heat contribution to the spectral distortions with Kompaneets equation [29] getting correctly the intermediate or *i*-type part of the distortion and use the actual *yim* and *ntr*-distortions for our COBE constraints.

At high redshifts($z \gtrsim 2 \times 10^5$), the Compton scattering process is very efficient and any initial distortion, including the *ntr*-type, thermalizes to a Bose-Einstein spectrum or μ-distortion irrespective of energy and type of injected particles [16]. At $z \lesssim 2 \times 10^5$, kinetic equilibrium is no longer possible and we must follow the full particle cascade to correctly calculate the final distortion.

We divide the energy range of interest into energy bins for each particle (e.g., photons, electrons, and positrons). The problem of electromagnetic cascade is then cast as a system of ordinary differential equations describing the flow of particles between different energy bins. This system can then be solved using the inductive approach [30–32]. Staring with an initial high energy particle, the electromagnetic cascade proceeds by sharing the total energy with more and more background particles, quickly multiplying the number of energetic particles (i.e., with energy *much* greater than the background electrons and photons). Since, the energy cascade is one-way (i.e., higher to low energy), solution for a given energy bin only depends on the cascade solution for the lower energy bins. Therefore, starting with the lowest energy bins, we can solve for populations of higher and higher energy bins in the cascade. Details of our numerical codes implementing the above method are described in detail in [20].

The inductive approach is an exact solution to the evolution equations under the assumption that a particle in a particular energy bin can only scatter to a lower energy bin. This is true as long as the thermal energies of CMB photons and background electrons can be neglected at desired numerical accuracy. Once this is no longer valid,

which happens when the particles have become nonrelativistic, we evolve the full Kompaneets equation which takes into account thermal distribution of background particles and scattering of particles into higher energy bins. Our approximations are therefore driven by desired numerical accuracy and not by ad hoc assumptions about the physics. In this sense our calculations are exact. Previous constraints were based on *yim*-distortions which are the solutions of Kompaneets equation valid only in the nonrelativistic limit. Therefore, the previous constraints are inaccurate since they use nonrelativistic solutions even when the injected particles are relativistic. We should emphasize that we use Kompaneets equation only when the energies of photons and electrons are much smaller than the electron mass and the conditions for the validity of Kompaneets equation are satisfied.

In an ionized universe, the most important scattering process for low energy electrons($\lesssim$keV) is Coulomb scattering and results in thermalization of the electron with most of its energy going to heat or *yim*-type distortions. The dominant energy loss mechanism for a relativistic electron or positron is elastic scattering (inverse Compton) with the CMB. Once a positron becomes nonrelativistic it annihilates with a background electron to give two 511 keV photons. The injection of a positron is therefore, to a very good approximation, equivalent to an electron with same initial kinetic energy and two 511 keV photons. Since, the energy loss rates for electrons and positrons are extremely rapid compared to Hubble scale, they deposit their energy instantaneously [20,30].

For photons, the relevant scattering processes are Compton scattering, pair production, and photon-photon elastic scattering. For most of the relevant energy range, the energy loss rate for photons is comparable to the Hubble rate. Therefore, we evolve the photon spectrum with background expansion taken into account. The most important process which determines the shape of the spectral distortion is elastic or Compton scattering of photons and electrons. Energetic photons produce energetic electrons and energetic electrons produce energetic photons by Compton scattering. The cycle repeats until the electrons start losing energy by Coulomb scattering to heat or loss of energy by photons in Compton scattering ($\propto \nu/m_e$, where ν is the photon frequency and m_e is the electron mass) becomes inefficient, i.e., the spectral distortion is frozen. Initial $\sim$10 keV electrons will just produce a spectral distortion with significant high energy Wien tail ($x = h\nu/(k_B T) \gtrsim 20$), where h is Planck's constant and k_B is the Boltzmann constant, and T is CMB temperature) compared to *yim*-distortions. As we increase the energy of initial particles, they lose energy in smaller number of scatterings, giving a smaller amplitude in the CMB band and more photons at higher and higher energies in the Wein tail. The highest energy photons in the distortion will however lose their energy to background electrons which will upscatter CMB and increase the amplitude of the distortion in the main CMB band. Thus the energy from the highest energy photons in the CMB spectral distortion cycles back to the main CMB band ($x \lesssim 20$). The amplitude of the distortions in the main CMB band therefore oscillates as we increase energy of injected particles or the dark matter mass. In addition, due to the cyclical production of energetic electrons and photons, for very high energy ($\gtrsim$10 GeV) electron injection and photon injection become indistinguishable [20,30].

III. SPECTRAL DISTORTIONS FROM DARK MATTER DECAY INTO PHOTONS AND ELECTRON-POSITRON PAIRS

We can write the energy density (E) injection rate for particle decay as

$$\frac{dE}{dt} = \frac{f_X \rho_{\rm DM}}{\tau_X} \exp(-t/\tau_X) \tag{3.1}$$

where τ_X is the particle decay lifetime and z_X is the redshift at proper time $t = \tau_X$, $\rho_{\rm DM}(z) = (1+z)^3 \rho_{\rm DM}(z=0)$ is the nondecaying dark matter energy density at redshift z and f_X is ratio of the initial energy density of decaying dark matter to that of the nondecaying component.

We plot the energy density deposited as heat for 20 GeV dark matter decaying into 10 GeV electron-positron pairs per logarithmic redshift interval as a fraction of the CMB energy density (ρ_γ) with full evolution of particle cascades in Fig. 1 and compare it with the "*yim*-approximation," i.e., instantaneous deposition of all energy as heat for $f_X = 0.0003$. There is a clear time delay between energy injection and deposition as heat in the exact calculation and there is a bias in the temporal information also in the *yim*-approximation.

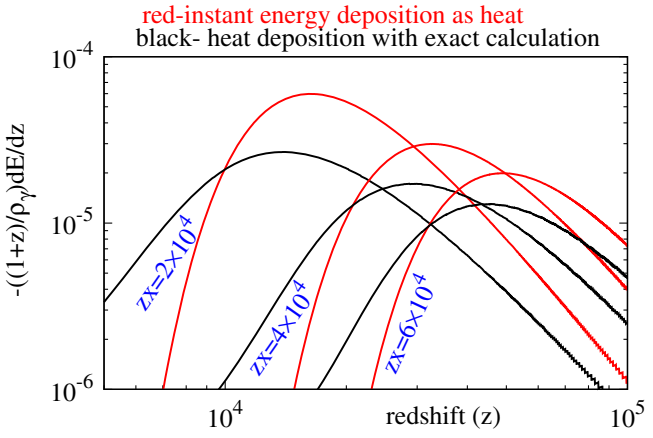

FIG. 1. Ratio of energy density deposited as heat with respect to CMB energy density for varying z_X and $f_X = 0.0003$ for 20 GeV dark matter decay into monochromatic electron-positron pairs.

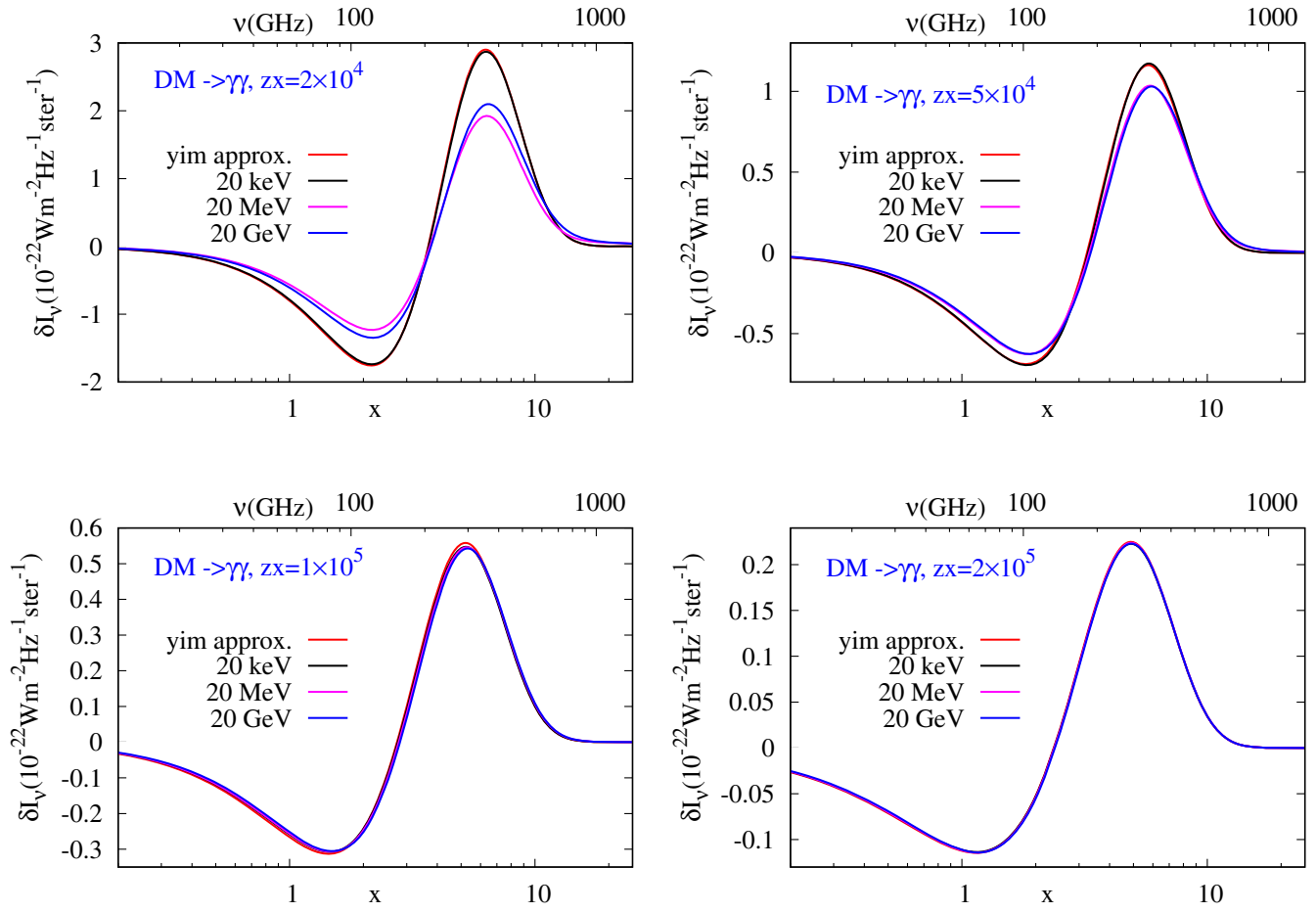

FIG. 2. Spectral distortions for dark matter decay into monochromatic photons for different m_X and z_X and constant $f_X = 0.0003$.

In Fig. 2, we plot the spectral distortions for dark matter decaying to two monochromatic photons and compare our exact calculations with the spectral distortion in the *yim*-approximation, the latter being insensitive to the mass of dark matter. In our new calculation we find that the amplitude of the distortion is very sensitive to the mass of the dark matter, especially at low redshifts. The difference in shape is most evident in the high frequency tail of the spectral distortion. As we increase the redshift, the sensitivity to the initial dark matter mass decreases and the spectral distortion becomes closer to the *yim*-approximation, the two becoming indistinguishable and close to a Bose-Einstein spectrum (μ-distortion) at $z_X \gtrsim 2 \times 10^5$.

To see the difference between our new calculations and the *yim*-distortions, we fit the *yim*-distortions to our solutions for a PIXIE like experiment [33]. We fit the sum of y-type, μ-type, i-type at redshift 20000, and a temperature shift (see Appendix C of [20]) with the amplitude of the four spectra as free parameters. For the fit we sample the distortions at equally spaced PIXIE channels from 30 GHz to 600 GHz with 15 GHz spacing between the channels. The results of such a fit are shown in Fig. 3 for some of the decay channels shown in Fig. 2 for decaying dark matter with decay redshift $z_X = 2 \times 10^4$. We also show the residuals which are the difference between our calculation and the best fit *yim*-distortions. The residuals are especially large at high frequencies as can be already seen in Fig. 2. The presence of high frequency channels and efficient removal of high frequency foregrounds will therefore be important for detecting the nonthermal distortions in the future experiments.

As long as we do not have a detection but only upper limits, we can get conservative limits by considering only one type of distortion at a time. This is for example also done by the COBE-FIRAS [8] team when they give limits on y and μ-type distortions separately. However, once we have a positive detection of distortion there will be degeneracy between postrecombination and prerecombination distortions. The only way such a degeneracy can be broken is if we can detect the nonthermal part of the prerecombination distortions. This approach will however not work for the *yim*-distortions, e.g., from Silk damping [34,35]. Another way would be using 21 cm observations to learn about the reionization epoch and subtract the reionization contribution. Prerecombination distortions would also modify the cosmological recombination

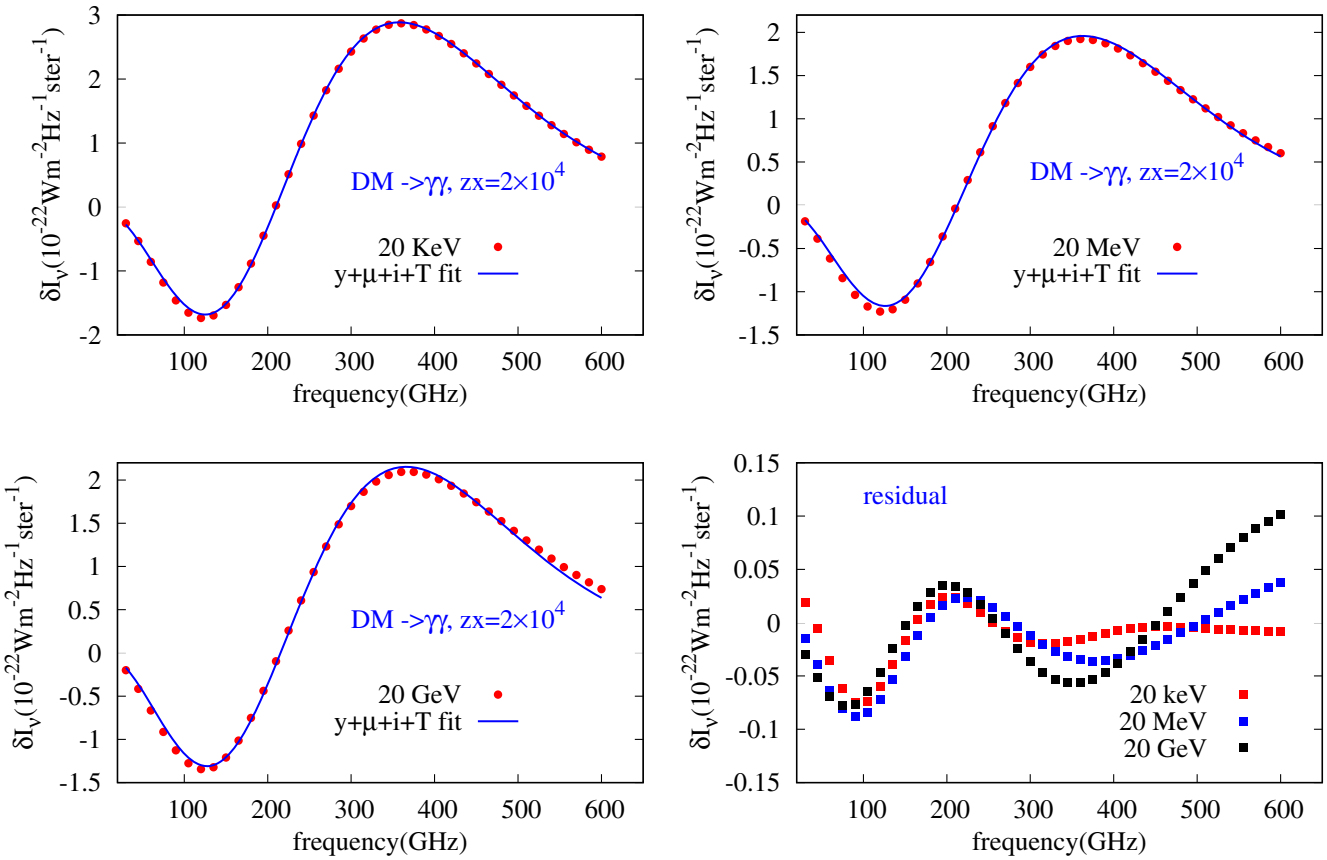

FIG. 3. Best thermal distortion fit to actual distortion spectral and corresponding residual for decaying dark matter of lifetime $z_X = 20000$.

spectrum and can in principle be used to constrain prerecombinational energy injection [36].

We use COBE-FIRAS data [8], publicly available on the NASA LAMBDA website,[1] to constrain the fraction of dark matter that can decay as a function of decay redshift z_X. We use the same procedure that was used by [8] for the μ-type distortion and simultaneously fit the spectral distortion from decay, a temperature shift and the galactic spectrum given in Table 4 of [8] to the COBE-FIRAS monopole residuals. We do not find any positive detection and plot 95% upper limits for f_X in Fig. 4 for dark matter decaying to monochromatic photons and electron-positron pairs. We also show constraints in the *yim*-approximation.

If we assume that all energy goes into the spectral distortion with fixed shape, e.g., a μ-type distortion, then the amplitude of the distortion will just be proportional to $f_X\rho_{\rm DM}/\rho_\gamma \propto f_X/(1+z_X)$. At higher redshifts the decay of same amount of dark matter will give a smaller distortion because the energy density of CMB is higher by a factor of $(1+z_X)$. For a given sensitivity of the experiment, the constraints on f_X become weaker with redshift, $\propto(1+z_X)$, with some correction because the decay does not happen instantaneously. This is what we see in the curve labeled *yim*-approximation. Since we take into account that the distortion at $z \lesssim 2\times 10^5$ is not exactly μ but i-type and becomes y-type at $z \sim 10^4$, there is a small departure from this linear relation. For our exact calculation, explicitly evolving the electromagnetic cascade, there is dramatic departure from the *yim*-approximation, with the difference of a factor of 4.7 for electron-positron channel for $m_X \approx 4$ MeV and a factor of 4.1 for the photon channel for $m_X \approx 3$ MeV at $z_X \approx 5000$ or dark matter lifetime $\tau_X = 8\times 10^{11}$ s. As we go to higher redshifts, the constraints become closer to the *yim*-approximation as Compton scattering become more efficient in reprocessing the energy trying to establish a Bose-Einstein spectrum. The constraints in particular are very sensitive to the mass of the decaying particle.

We show our new constraints from full evolution of electromagnetic cascades in the $m_X - z_X, \tau_X$ plane in Fig. 5 for decay to photons and electron-positron pairs. The color scale represents the 95% upper limits on f_X from COBE-FIRAS data. In the *yim*-approximation there will be no sensitivity to m_X and the isocontours of f_X would all be vertical lines. This is what we see at high redshifts, where *yim*-approximation holds. At lower redshifts the spectral distortions and hence the constraints become sensitive to m_X. The cyclic nature of electromagnetic cascades, as

[1]https://lambda.gsfc.nasa.gov/product/cobe/firas_products.cfm

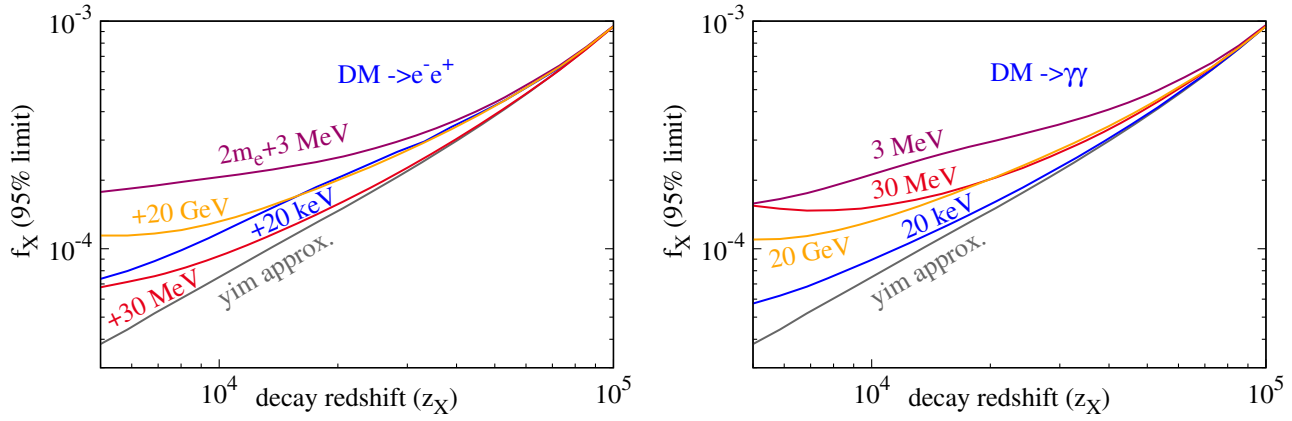

FIG. 4. 95% COBE-FIRAS upper limits on f_X for different m_X as a function of decay redshift z_X. Also shown is the constraint in the *yim*-approximation.

discussed above, is reflected in oscillation in the isocontours in the m_X direction. At $z \approx 2 \times 10^6$ the photon creation processes, double Compton scattering and bremsstrahlung, become important suppressing the spectral distortions [1,2] and weakening the constraints. We have taken this suppression into account using the blackbody visibility function from [4].

We should also mention that there are existing constraints from big bang nucleosynthesis (BBN) with explicit evolution of electromagnetic cascades [37–41] for decaying dark matter with the same lifetimes as are considered in this paper. We refer the reader to Fig. 9 of [41] for a comparison of constraints obtained from spectral distortions and BBN. For photon injections with energy close to photo-dissociation threshold of deuterium ($\lesssim$10 MeV), the constraints from spectral distortions are stronger compared to BBN. This is because these photons immediately scatter with the background electrons dividing their energy into lower energy photons below the deuterium dissociation threshold of 2.2 MeV and are therefore unable to dissociate deuterium nuclei. As we increase the energy of the injected photons, more and more photons will be able to dissociate deuterium and, for high enough energy, helium nuclei. Hence constraints from BBN are stronger for photon injection with energies $\gtrsim$10 MeV. For electron-positron pair injection in the energy range 10 MeV-100 MeV, the low energy photons produced by inverse Compton scattering are below the deuterium dissociation threshold, though there are some high energy photons produced by the final state radiation. For higher energies, we expect the constraints from e^-e^+ to be stronger than spectral distortion constraints and follow similar patterns as for the photon injection (e.g., see Fig. 13 of [38]). Since, with our detailed calculations, constraints from spectral distortions are relaxed, for most of the energy range, constraints from BBN are still stronger compared to spectral distortion with present data. Future experiments will improve the spectral distortion constraints by many orders of magnitude and accurate calculations such as ours are essential to make the science case and to arrive at the minimum improvement in sensitivity that will be necessary to beat the BBN constraints.

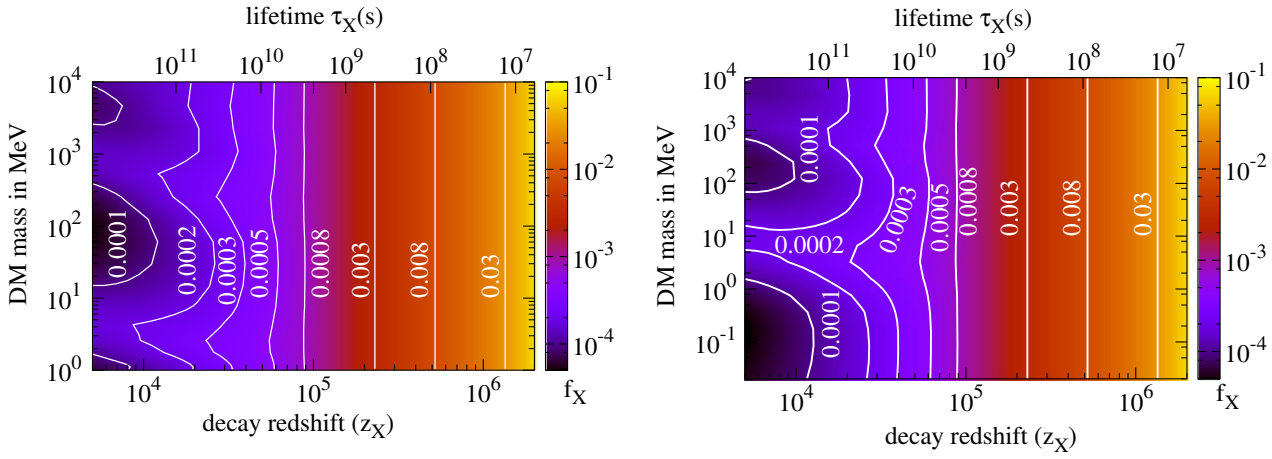

FIG. 5. 95% COBE-FIRAS limits on f_X for decay into electron-positron pairs (left) and photons (right).

IV. CONCLUSIONS

We have derived new upper limits on dark matter decay in the early Universe from COBE-FIRAS measurements of the CMB monopole spectrum. We explicitly evolve the electromagnetic cascades resulting from dark matter decay into photons and electron-positron pairs, calculate the resulting spectral distortions in the CMB band and use these to constrain the dark matter decay into these two channels. Previous COBE constraints have assumed that all energy from decay goes into heat and gives y-type and μ-type distortions and were therefore blind to the decay channel. We show that these approximations fail at low redshifts, $z_X \lesssim 2 \times 10^5$ or dark matter lifetimes $\tau_X \gtrsim 6 \times 10^8$ s. In addition, the spectral distortions, and hence the constraints, are sensitive to the dark matter mass. Our results show that the decay channels are important for spectral distortions, just as they are important for the CMB recombination history for larger lifetimes [42–45]. This work motivates a more comprehensive study, in the future, taking into account different decay channels motivated by different particle physics models in specific cosmological scenarios such as in [11]. Future experiment like Primordial Inflation Explorer (PIXIE) [33] would have a sensitivity of 3-4 orders of magnitude better than COBE-FIRAS [46] and may discover distortions from new physics in the early Universe. Accurate calculations of spectral distortions by explicitly evolving the electromagnetic cascades would be crucial in interpretation of such a future detection.

ACKNOWLEDGMENTS

This work was supported by Science and Engineering Research Board, Department of Science and Technology, Govt. of India Grant No. ECR/2015/000078. This work was also supported by Max Planck Partner Group between Tata Institute of Fundamental Research, Mumbai and Max-Planck-Institut für Astrophysik, Garching funded by Max-Planck-Gesellschaft.

[1] R. A. Sunyaev and Y. B. Zeldovich, The interaction of matter and radiation in the hot model of the Universe, II, Astrophys. Space Sci. **7**, 20 (1970).
[2] L. Danese and G. de Zotti, Double Compton process and the spectrum of the microwave background, Astron. Astrophys. **107**, 39 (1982).
[3] J. Chluba and R. A. Sunyaev, The evolution of CMB spectral distortions in the early Universe, Mon. Not. R. Astron. Soc. **419**, 1294 (2012).
[4] R. Khatri and R. A. Sunyaev, Creation of the CMB spectrum: Precise analytic solutions for the blackbody photosphere, J. Cosmol. Astropart. Phys. 06 (2012) 038.
[5] Y. B. Zel'dovich, V. G. Kurt, and R. A. Syunyaev, Recombination of hydrogen in the hot model of the Universe, Sov. J. Exp. Theor. Phys. **28**, 146 (1969).
[6] P. J. E. Peebles, Recombination of the primeval plasma, Astrophys. J. **153**, 1 (1968).
[7] J. C. Mather *et al.*, Measurement of the cosmic microwave background spectrum by the COBE FIRAS instrument, Astrophys. J. **420**, 439 (1994).
[8] D. J. Fixsen, E. S. Cheng, J. M. Gales, J. C. Mather, R. A. Shafer, and E. L. Wright, The cosmic microwave background spectrum from the full COBE FIRAS data set, Astrophys. J. **473**, 576 (1996).
[9] W. Hu and J. Silk, Thermalization Constraints and Spectral Distortions for Massive Unstable Relic Particles, Phys. Rev. Lett. **70**, 2661 (1993).
[10] J. L. Feng, A. Rajaraman, and F. Takayama, Superweakly interacting massive particle dark matter signals from the early Universe, Phys. Rev. D **68**, 063504 (2003).
[11] E. Dimastrogiovanni, L. M. Krauss, and J. Chluba, Constraints on gravitino decay and the scale of inflation using CMB spectral distortions, Phys. Rev. D **94**, 023518 (2016).
[12] R. A. Sunyaev and R. Khatri, Unavoidable CMB spectral features and blackbody photosphere of our Universe, Int. J. Mod. Phys. D **22**, 1330014 (2013).
[13] Y. B. Zeldovich and R. A. Sunyaev, The interaction of matter and radiation in a hot-model Universe, Astrophys. Space Sci. **4**, 301 (1969).
[14] A. F. Illarionov and R. A. Siuniaev, Comptonization, the background-radiation spectrum, and the thermal history of the universe, Sov. Astron. **18**, 691 (1975).
[15] C. Burigana, L. Danese, and G. de Zotti, Formation and evolution of early distortions of the microwave background spectrum–A numerical study, Astron. Astrophys. **246**, 49 (1991).
[16] R. Khatri and R. A. Sunyaev, Beyond y and μ: The shape of the CMB spectral distortions in the intermediate epoch, $1.5 \times 10^4 \lesssim z \lesssim 2 \times 10^5$, J. Cosmol. Astropart. Phys. 09 (2012) 016.
[17] J. Chluba, Green's function of the cosmological thermalization problem, Mon. Not. R. Astron. Soc. **434**, 352 (2013).
[18] R. Khatri and R. A. Sunyaev, Forecasts for CMB μ and i-type spectral distortion constraints on the primordial power spectrum on scales $8 \lesssim 10^4$ Mpc^{-1} with the future Pixie-like experiments, J. Cosmol. Astropart. Phys. 06 (2013) 026.
[19] J. Chluba and D. Jeong, Teasing bits of information out of the CMB energy spectrum, Mon. Not. R. Astron. Soc. **438**, 2065 (2014).
[20] S. K. Acharya and R. Khatri, Rich structure of nonthermal relativistic CMB spectral distortions from high energy

particle cascades at redshifts $z \lesssim 2 \times 10^5$, Phys. Rev. D **99**, 043520 (2019).
[21] J. L. Feng, A. Rajaraman, and F. Takayama, Superweakly Interacting Massive Particles, Phys. Rev. Lett. **91**, 011302 (2003).
[22] J. L. Feng, Dark matter candidates from particle physics and methods of detection, Annu. Rev. Astron. Astrophys. **48**, 495 (2010).
[23] B. J. Carr, K. Kohri, Y. Sendouda, and J. Yokoyama, New cosmological constraints on primordial black holes, Phys. Rev. D **81**, 104019 (2010).
[24] M. Ricotti, J. P. Ostriker, and K. J. Mack, Effect of primordial black holes on the cosmic microwave background and cosmological parameter estimates, Astrophys. J. **680**, 829 (2008).
[25] D. Aloni, K. Blum, and R. Flauger, Cosmic microwave background constraints on primordial black hole dark matter, J. Cosmol. Astropart. Phys. 05 (2017) 017.
[26] Y. Ali-Haïmoud and M. Kamionkowski, Cosmic microwave background limits on accreting primordial black holes, Phys. Rev. D **95**, 043534 (2017).
[27] R. Khatri and R. A. Sunyaev, Time of primordial ^{7}Be conversion into ^{7}Li, energy release and doublet of narrow cosmological neutrino lines, Astron. Lett. **37**, 367 (2011).
[28] N. Aghanim *et al.*, Planck 2018 results. VI. Cosmological parameters, arXiv:1807.06209.
[29] A. S. Kompaneets, The establishment of thermal equilibrium between quanta and electrons, J. Exp. Theor. Phys. **31**, 876 (1956).
[30] T. R. Slatyer, N. Padmanabhan, and D. P. Finkbeiner, CMB constraints on WIMP annihilation: Energy absorption during the recombination epoch, Phys. Rev. D **80**, 043526 (2009).
[31] T. Kanzaki and M. Kawasaki, Electron and photon energy deposition in the Universe, Phys. Rev. D **78**, 103004 (2008).
[32] T. Kanzaki, M. Kawasaki, and K. Nakayama, Effects of dark matter annihilation on the cosmic microwave background, Prog. Theor. Phys. **123**, 853 (2010).
[33] A. Kogut, D. J. Fixsen, D. T. Chuss, J. Dotson, E. Dwek, M. Halpern, G. F. Hinshaw, S. M. Meyer, S. H. Moseley, M. D. Seiffert, D. N. Spergel, and E. J. Wollack, The primordial inflation explorer (PIXIE): A nulling polarimeter for cosmic microwave background observations, J. Cosmol. Astropart. Phys. 07 (2011) 025.
[34] J. Chluba, R. Khatri, and R. A. Sunyaev, CMB at 2×2 order: The dissipation of primordial acoustic waves and the observable part of the associated energy release, Mon. Not. R. Astron. Soc. **425**, 1129 (2012).
[35] R. Khatri, R. A. Sunyaev, and J. Chluba, Mixing of blackbodies: Entropy production and dissipation of sound waves in the early Universe, Astron. Astrophys. **543**, A136 (2012).
[36] J. Chluba and R. A. Sunyaev, Pre-recombinational energy release and narrow features in the CMB spectrum, Astron. Astrophys. **501**, 29 (2009).
[37] M. Kawasaki, K. Kohri, and T. Moroi, Big-bang nucleosynthesis and hadronic decay of long-lived massive particles, Phys. Rev. D **71**, 083502 (2005).
[38] M. Kawasaki, K. Kohri, T. Moroi, and Y. Takaesu, Revisiting big-bang nucleosynthesis constraints on long-lived decaying particles, Phys. Rev. D **97**, 023502 (2018).
[39] V. Poulin and P. D. Serpico, Nonuniversal BBN bounds on electromagnetically decaying particles, Phys. Rev. D **91**, 103007 (2015).
[40] M. Hufnagel, K. Schmidt-Hoberg, and S. Wild, BBN constraints on MeV-scale dark sectors. Part II: Electromagnetic decays, J. Cosmol. Astropart. Phys. 11 (2018) 032.
[41] L. Forestell, D. E. Morrissey, and G. White, Limits from BBN on light electromagnetic decays, J. High Energy Phys. 01 (2019) 074.
[42] J. A. Adams, S. Sarkar, and D. W. Sciama, Cosmic microwave background anisotropy in the decaying neutrino cosmology, Mon. Not. R. Astron. Soc. **301**, 210 (1998).
[43] X. Chen and M. Kamionkowski, Particle decays during the cosmic dark ages, Phys. Rev. D **70**, 043502 (2004).
[44] T. R. Slatyer and C.-L. Wu, General constraints on dark matter decay from the cosmic microwave background, Phys. Rev. D **95**, 023010 (2017).
[45] V. Poulin, J. Lesgourgues, and P. D. Serpico, Cosmological constraints on exotic injection of electromagnetic energy, J. Cosmol. Astropart. Phys. 03 (2017) 043.
[46] D. J. Fixsen and J. C. Mather, The spectral results of the far-infrared absolute spectrophotometer instrument on COBE, Astrophys. J. **581**, 817 (2002).